The Influence of Salt Concentration in Injected Water on Low-Frequency Electrical-Heating-Assisted Bitumen Recovery

I.I. Bogdanov, J.A. Torres, H.A. Akhlaghi, and **A.M. Kamp,** SPE, CHLOE, University of Pau, France

Summary

Steam injection is often not a good alternative for oil recovery from shallow bitumen reservoirs. For instance, the thin caprock creates the danger of steam breakthrough. For deeper reservoirs, the heat losses from injection wells may be prohibitive. A technology that may be better suited is oil recovery aided by low-frequency electrical heating of the reservoir. This technology, well known for environmental remedial applications, has been field tried recently, yielding promising results. The process uses electric conductivity of connate water to propagate an alternating current between electrodes, inducing the Joule heating of the reservoir. An associated problem is the appearance of hot spots around the electrodes that may be relieved by water circulation. However, the water circulation may have a significant effect on the heating process because the electric conductivity of the circulated water depends on its salt content.

To find out the influence of salt concentration on process efficiency, we have studied the process of salt-water recirculation around an electrode using numerical simulation. The physical properties and operational data for Athabasca bitumen have been collected from the literature. The model built with Computer Modelling Group's STARS simulator and tested first with available analytical solutions has been validated, and the proper choice of the underlying grid and numerical tuning parameters has been verified. The process was also simulated at field scale for a common pattern of electrodes and production wells. The salt penetrated into the reservoir, far beyond the major water-circulation zone around the electrodes. This process increases the electric conductivity in a large region between electrodes, which improves the heating of the reservoir. The single-electrode simulation studies using different tools yielded similar results for a simple problem. More-complex (and more-realistic) field-scale simulations show that adding salt enhances the oil production. In practice, an upper concentration limit may be given by corrosion problems at the electrodes.

The reservoir simulation of bitumen recovery assisted by low-frequency heating is a challenging multiphysics problem. The understanding of the influence of salt concentration on the circulated water provided by this work is an important key in process-design considerations.

Introduction

The common objective of thermal-recovery methods applied to heavy-oil and oil-sand deposits is to enhance the oil-recovery process. Oil sands are a mixture of sand, water, and bitumen, in which the oil API gravity is less than 10°API. There are vast bitumen extraheavy-oil reservoirs in Canada and Venezuela. As an example, the Alberta Energy and Utilities Board estimates that, under current technology, more than 300 billion bbl are recoverable from the Alberta oil sands (McGee and Vermeulen 2007). Generally, the basic mechanism of thermal-recovery processes is to increase the reservoir temperature and thereby reduce the oil viscosity to make mobile the original oil (bitumen) in the reservoir.

Methods of heating the reservoir oil include well-known fluid-injection methods such as cyclic steam stimulation, steamflooding, steam-assisted gravity drainage (SAGD), fire flooding, and newer techniques of in-situ reservoir heating with electromagnetic energy. Steam-injection and fire-flooding techniques are now applied commercially to heavy-oil deposits, but they are technically difficult and uneconomical in some oil-sand deposits with very viscous oil. All fluid-injection methods in oil-sand deposits encounter the same problems of very low initial injectivity, poor communication between the wells and poor control of injected-fluid movement, reservoir heterogeneity, and unfavorable mobility ratio, leading to poor sweep efficiency (Hiebert et al. 1986). The shallow depth of Canadian reservoirs is another limitation for the steam-injection methods, such as SAGD, which are more appropriate for deep reservoirs. For example, besides the elevated probability of steam leakage, there is a likelihood of formation fracturing with the use of high injection pressures.

Low-Frequency Electrical Heating. One of the methods of in-situ heat generation that overcomes these difficulties, at least partially, is the electrical-heating method that has been developing for approximately 30 years and has already been tested at large scale. To heat the reservoir with this method, there is no need for fluid injection, so the problems of low injectivity, communication paths, and poor mobility ratio, which are common for other heating methods, do not occur. Also, reservoir depth and thickness are not limiting factors for electrical heating. This method can also be used to mobilize the original oil as a preheating technology for subsequent steamdrive processes. The electrical-heating methods can be divided into three different groups: high-frequency heating ($> 10^6$ Hz), induction, and low-frequency heating (typically 50–60 Hz). The subject of this work is the numerical study of the low-frequency-heating (LFH) method.

From a physical viewpoint, the LFH method is based on the Joule effect of the circulating electric current, the conducting path for electrical current being through the continuous connate water enveloping the nonconductive sand particles. Electrical energy is converted into heat along these pathways because of the electrical resistivity of the water, and the heat is transferred to the oil and the sand particles by conduction. The temperature is increased over the reservoir volume because of the heat generation, and then the variations of fluid (mainly water) saturation and temperature affect the bulk electrical conductivity of the reservoir.

Recent LFH Activity Review. Numerous efforts were made in the last several decades to develop reliable laboratory experiments, simulation tools, and pilot tests of recovery processes for LFH. In this subsection, a brief survey of this work is made—in particular, paying attention to details of the recurrent idea of combining electrical heating with water injection. The advantages of this approach are the control of electrode temperature to avoid water evaporation at hot spots in the vicinity of electrodes, the improvement of heating accomplished by means of enhancement of heat

Copyright © 2011 Society of Petroleum Engineers

This paper (SPE 129909) was accepted for presentation at the SPE Symposium on Improved Oil Recovery, Tulsa, 24–28 April 2010, and revised for publication. Original manuscript received for review 23 February 2010. Revised manuscript received for review 16 July 2010. Paper peer approved 16 September 2010.

transfer, and the modification of bulk electrical conductivity by injecting salt water; the latter results in effective expansion of the elevated-conductivity region.

The idea of the heating improvement by increasing bulk electrical conductivity through the use of salty brine was first presented by El-Feky (1977) and then by Harvey et al. (1979). They investigated the feasibility of using an electric current for the selective heating of portions of an oil reservoir. A set of laboratory experiments was conducted to determine oil recovery from a five-spot pattern combining waterflooding with electrical heating. To augment the effect of applied potential, they performed a preliminary injection of an NaCl aqueous solution of 200,000 ppm. Finally, the oil recovery was 13% greater with selective heating than with the waterflood alone.

Todd and Howell (1978) developed a radial model to evaluate the electrical-potential distribution, the temperature distribution, the heat flow, and the single-phase flow produced by thermal expansion of reservoir fluids under electrical heating. They examined the effects of resistivity, wellbore size, well-cooling temperature, and well spacing. They demonstrated that it is possible to maintain the same total energy dissipated into the reservoir for three different levels of initial resistivity (23, 100, and 200 Ω·m) by adjusting the electrical potential. The mean temperature-rise rate (TRR) was approximately 0.2–0.3°C/d. It was found that increasing the effective electrode radius from 5 to 10 ft may lead to faster heating. Also, they pointed out that increasing the well spacing from 75 to 100 ft can lead to a larger reservoir volume to heat electrically, which, in turn, increases the energy demand approximately 43% for the case under consideration.

Later, Hiebert et al. (1986) developed a code based on a finite-difference model that was used for simulations of the electric-preheat steamdrive process. With the help of this simulation tool, Hiebert et al. (1989) showed that electrical preheating can establish a fluid communication path between injector and producer wells in a typical Athabasca formation and also may help to establish some injectivity. The electrical preheating period consists of applying a constant power of 1.45 MW to the five-spot pattern for 1 year. The following period consisted of no heating with closed wells for 2 weeks and then a steamdrive phase consisting of a sequence of steam and hot-water injections over 3,000 days. The total oil recovery was 59% of the original oil in place. Under the conditions studied, after completing the preheating period, the mean TRR observed is in the range 0.03–0.3°C/d (depending on the dimensions of the model), while the maximum rate is approximately 0.1–1°C/d.

Alternatively, Killough and Gonzales (1986) developed a fully implicit, 3D multicomponent reservoir simulator capable of treating the effect of the variation of bulk reservoir electrical conductivity on temperature, water saturation, and salt content. They validated their simulator using the laboratory results of El-Feky (1977) and with analytical models. This simulator was applied to evaluate the possibility of conventional and nonconventional completion schemes, such as horizontal electrodes. They noticed the difficulties encountered by iterative solvers when trying to solve the linear system resulting from the application of finite differences to the coupled electrical/fluid-flow problem.

Pizarro and Trevisan (1990) carried out an interesting analysis of a pilot test in the Rio Panon field. In their work, the field data were matched by numerical simulations carried out with a numerical simulator developed by them. Original oil viscosity and temperature were approximately 2500 cp and 37°C, respectively. During a first stage of the preheating period, an average power level on the order of 20 kW was applied. After 40 days, the oil temperature at the wellbore increased to approximately 90°C, with a resulting rate of increase of 1.3°C/d. Then, during the second stage of the preheating period, the power level was augmented to 30 kW and the temperature rose to 100°C, with a rate of increase of 0.25°C/d. The history matching indicates the presence of an initial well damage that was gradually removed with the application of the electrical heating. Under the pilot-test conditions, the electrical heating worked more as a stimulation process rather than a recovery process.

McGee and Vermeulen (2007) presented a numerical study focused on the electrothermal dynamic stripping process (ETDSP) applied at reservoir conditions that are representative for the Athabasca oil sands. The ETDSP is stated to take advantage of a distributed voltage control between the electrode array and the water injection at the end of the electrodes. Water injection prevents boiling of the water phase and facilitates the heat distribution by flow convection mechanisms. The operation strategy consisted of three main stages: the first is a 30-day preheating period, followed by a 180-day heating/production stage, and ending with a 150-day period of production (without any electrical heating in order to take advantage of the residual heat from previous stages). The oil-production peak was observed at the beginning of the second stage, and the TRR was approximately 2°C/d. The authors concluded that the recovery factor was comparable with a successful SAGD project.

McGee (2008) published the results of the first ETDSP pilot test carried out from September 2006 to August 2007. Initially, the operation strategy was similar to that proposed in the theoretical study (McGee and Vermeulen 2007) except for the electrode spacing (8 m instead of 16 m). The major variation from the original project was the replacement of reciprocating pumps by progressing-cavity pumps, which led to successful production of very viscous oil (approximately 10^5 cp). Also, the total amount of energy injected into the reservoir was 25% less than the target total energy because many of the electrodes failed during the operation. The mean temperature obtained from measurements after completing the preheating stage was similar to that predicted by theory (i.e., with an average rate of increase of approximately 2°C/d). Also, the peak temperatures of 75–80°C were consistent with the numerical model. Finally, the estimated recovery factor was approximately 75%.

According to references already mentioned (McGee 2008; McGee and Vermeulen 2007), the order of magnitude for the TRR during the preheating period seems to be consistently in the range of 0.1–1°C/d. On the other hand, the bulk reservoir electrical conductivity depends strongly on the water saturation and the salt concentration in the water phase. The electrical potential may be adjusted to provide the necessary power supply and to compensate low bulk electric conductivity.

The Water-Circulation Effect. The reservoir-water evaporation that occurs around the electrodes because of the generation of high-temperature spots is one of the important problems of the electrical-heating method. This phenomenon cuts the conductive paths near the electrode and sharply decreases the efficiency of the process. In order to improve the heat distribution in the reservoir during the low-frequency electrical heating, the water can be recycled around the electrode (McGee and Vermeulen 2007). The water circulation can absorb the heat in the electrode's vicinity and prevent evaporation of reservoir water, which may allow operation at larger energy-input level. Water circulation (more generally, the transportation of water away from an electrode) also leads to more-homogeneous heat distribution in the reservoir because of convective heat transfer around the electrode.

The other advantage of the water circulation, related to reservoir electrical properties, is increasing the bulk electrical conductivity in the reservoir, especially around the injection well (electrode), according to Archie's law. Reservoir electrical conductivity plays an important role in heat generation at low-frequency electrical heating. At similar applied potential input, a reservoir with higher electrical conductivity generates more electric power.

So the water circulation is a suitable way for achieving conductivity enhancement, and particularly using salt water (brine) instead of fresh water. The effect of the brine injection on bitumen recovery during LFH—which can result, for example, from expected lower electric potential applied per unit of power supply, shorter preheating time, and lower heat losses—is the main subject of our current work. The LFH study including coupled electrothermal and fluid dynamic transfer phenomena has been made by means of numerical modeling on the basis of available published information about the electrical and physical properties of bitumen reservoirs.

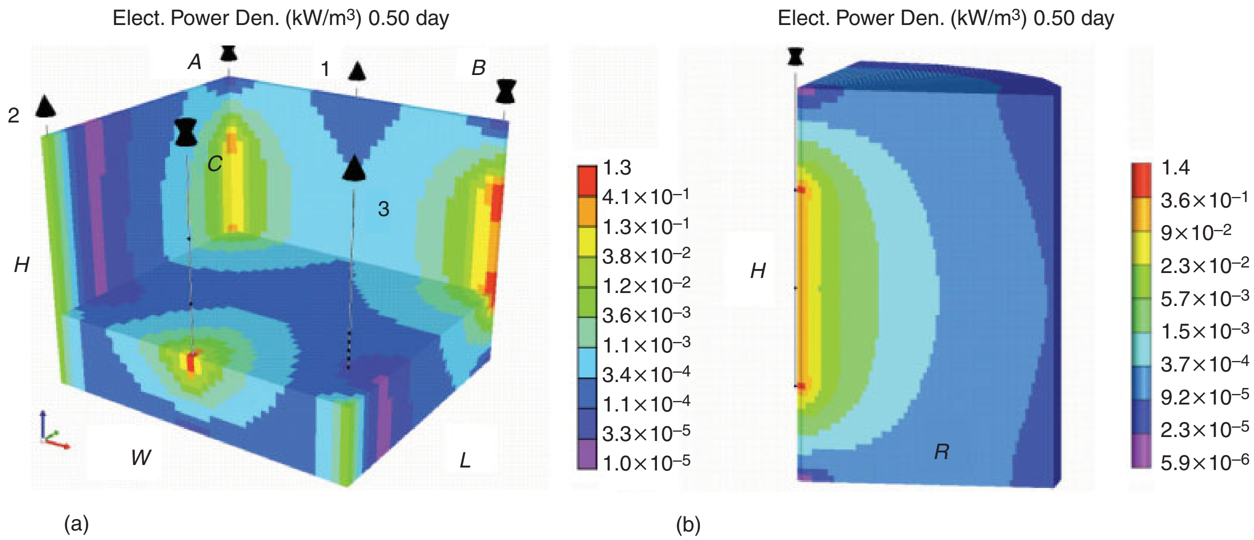

Fig. 1—Power fields at initial reservoir conditions in the case of the 3D radial model (b) and the base model (a). The regions sizes are *L*, *W*, and *H* (3D base model length, width, and thickness, respectively) and *H* and *R* (3D-radial-model thickness and horizontal size, respectively), where the electrode spacing *W* = 2*R*. Three-phase potential is applied at Electrodes A, B, and C. The ground potential is applied at Production Wells 1, 2, and 3. Applied potential magnitude is 250 V (a) and 200 V (b).

Physical Background of the LFH Method

Physically, the method is based on the Joule effect, with the original (connate) reservoir water playing a role of conductor. The electrical current is supplied by means of the electrodes settled directly inside the reservoir. An alternating- or direct-current-based power supply can be used for the heating purpose (McGee and Vermeulen 2007; Wittle et al. 2008). The heat is generated over the reservoir volume according to the local electric-current density and, hence, the local fluid composition and temperature field, which affect the bulk electrical conductivity of the reservoir (Ucok et al. 1980; Hiebert et al. 1986). So, an understanding of physical mechanisms of this oil-recovery method requires a study of the heat and mass transfer under the LFH conditions.

Space and Time Scales of the Temperature Variations. Viewed at the pore-scale, the electric current typically passes through the connate-water film covering the grains (McGee and Vermeulen 2007). Despite the space restriction of the Joule heat release, it can be shown that the temperature quickly becomes nearly uniform and the thermal-equilibrium assumption for a saturated porous medium holds for a wide range of reservoir conditions. The volume-averaged local heating power is defined according to Joule's law, as follows:

$$P_{LF} = \sigma|\vec{E}|^2, \quad \text{(1)}$$

where the bulk reservoir electric conductivity σ is used; the electric field E is conventionally defined by means of the electric potential v:

$$\vec{E} = -\nabla v. \quad \text{(2)}$$

Typically, industrial power systems use three-phase alternating-electric-current supply, which means that complex potential formulation must be used in Eq. 2.

Unlike what has been stated about the pore-scale temperature, at local reservoir scale, and especially in the vicinity of a single electrode, the temperature field is not uniform at all. Typically, during the LFH, so-called hot spots occur near electrodes. These are because of the nearly singular diverging heating power (see Eq. A-6 and the power fields for two models in **Fig. 1**). In practice, however, the temperature growth is reduced by conductive and convective heat transfer and is limited by water evaporation. Evaporation is strongly undesirable because the LFH is impossible without conductor (i.e., without liquid water) around the electrode. So, enhanced heat transfer is required to stabilize the electrode temperature and to ensure the electric current between the electrodes. For this purpose, McGee and Vermeulen (2007) proposed an electrode that can be installed directly in the well and is equipped with a water-injection facility. They discussed the advantages of enhanced convective heat transfer from water circulation around the electrode facility. The circulation not only provides temperature control but also leads to the modification of bulk electric conductivity because of the variation of water saturation and temperature.

The temperature field and flow pattern around the electrode under water-recirculation conditions probably require a separate study. The electric potential, the temperature, and, hence, the fluid properties (e.g., viscosity, density, relative permeabilities) undergo strong variations here, and the variable fluid/fluid and solid/fluid interactions at high oil-to-water viscosity ratio can affect the flow composition, flow regime, and Joule power field. A few preliminary results show the importance of such physical factors and mass-transfer mechanisms such as gravity and capillary effects, mechanical (convective) dispersion, and reservoir compressibility.

The electrode spacing (W = 2R; Fig. 1) is of fundamental importance for the LFH applications. First, it changes the typical process time ($t_D \sim R^2$) and the heating-power amplitude by means of the conductance factor G, giving the mean TRR (for the values definition, see Appendix A). Roughly, the mean reservoir TRR increases by one order of magnitude if the spacing decreases by 3 times. At the same time, the temperature drop across the reservoir ($T_D = \sigma_0 V_0^2/K$; see Appendix A), which is proportional to total electric power supply, is less dependent on spacing. This means that the variation of the well/electrode spacing does not improve the temperature contrast much; for real process improvement, it is not enough simply to change the total power. To avoid or smooth out the hot-spots effect (i.e., to provide more-uniform temperature distribution) additional efforts are required. One of possible approaches to improve the method is the brine-assisted LFH.

Reservoir Electric Conductivity. Consider now another key parameter for LFH, the bulk electric conductivity of the reservoir. At a given electrode pattern, the conductivity field completely defines the distribution of electric power and, hence, the results of the preheating and dramatically influences the oil production. According to the generalized Archie's law,

$$\sigma = \alpha S_w^n \phi^m \sigma_w f(T), \quad \text{(3)}$$

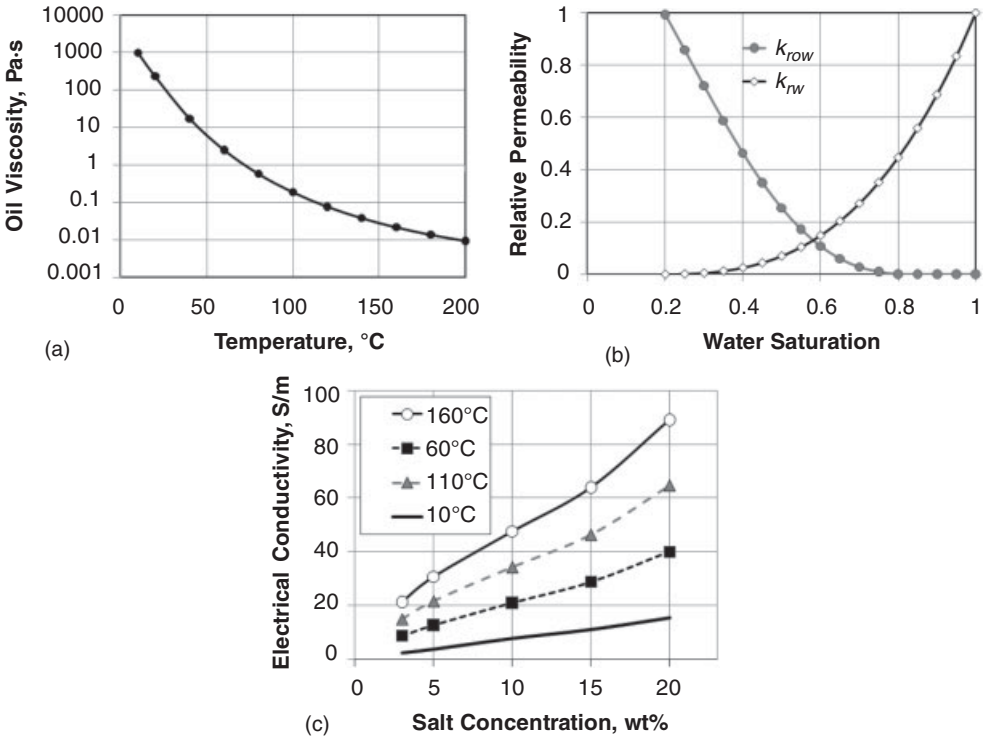

Fig. 2—Oil-viscosity temperature dependency (a), phase relative permeabilities (b), and water-phase electric-conductivity variation used in computations (Ucok et al. 1980; McGee and Vemeulen 2007); electric conductivity is given at different temperatures, specified in °C (c).

the bulk electric conductivity σ may vary with water saturation S_w, lithology type (the formation factor $F^{-1}=\alpha\phi^m$), temperature T, and with all factors affecting the water-phase (or brine) conductivity σ_w. The latter mainly include the effect of solutes dissolved in original and injected water. According to experimental data on the temperature dependency (Ucok et al. 1980; Hiebert et al. 1986), one may take as a general rule the nearly linear increase of the conductivity by a factor of approximately 3 for the first 100°C of temperature rise (see also the input data of simulations in **Fig. 2c**).

The variation of the water conductivity with the solute concentration depends much on the dissolved mineral. The choice of NaCl was both dictated by easy access and by its nearly constant solubility within a wide temperature range, which can be of crucial importance in view of solid precipitation at variable temperature. It is worth mentioning that the rate of water-conductivity increase with NaCl concentration is nearly constant and its order of magnitude value is 1 S/m per weight percent and more.

Given the applied potential, the influence of conductivity distribution on power can be estimated using a simple radial model of a composite medium (see Appendix A). The mean normalized power (which is the measure of the reservoir TRR) is defined by the electric-conductivity field and is depicted in **Fig. 3** (see Eq. A-11 for factor G and Eq. A-14 for the average heating power). Two remarks seem relevant here. The first is that the mean power varies relatively slowly, starting from some conductivity (graphs at κ = 30, 50, and 100 in Fig. 3). The second is that, to increase the initial mean power corresponding to uniform conductivity by a factor of 5–6, the bulk electric conductivity should be modified within a significant distance, which equals approximately 50% of the typical distance R. Note that, among the factors influencing the conductivity according to Archie's law (Eq. 3), only solute-concentration propagation may provide such a modification.

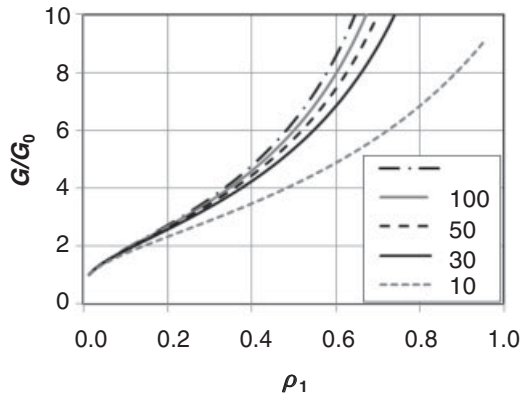

Fig. 3—Normalized conductance factor *G* for composite medium vs. elevated-conductivity-zone size (Eq. A-11).

The mechanisms of such propagation include convective, diffusive, and dispersive transport. The convection (by means of the water circulation) dominates near electrodes and also may become important after opening the production wells at elevated reservoir temperature. Taking into account that the conductivity-growth factor may be limited ($\kappa \approx 20$)—although, at the maximum solute concentration, this factor can be considerably greater—the diffusion, and especially the convective dispersion, may become important mechanisms of the solute propagation (or, more precisely, the propagation of an elevated-conductivity zone). Notice that the dispersion is proportional to local fluid velocitiy, so that this contribution to the conductivity modification can be controlled to some extent.

Conduction Dominating Early-Time Preheating. In the case of an extraheavy-oil or a bitumen reservoir, the injectivity at initial conditions is very low and injection of any fluid is nearly impossible. Technically, this very first period of heating is a difficult stage because of the limited brine-/water-circulation rate around the electrode, which does not facilitate control of both the electrode temperature and the circulation effect. To gain efficiency at this stage, it might be feasible to use conduction heat transfer as a principal mechanism for heating. To show this, compare conductive and Joule's-power-source terms in the heat energy-balance equation (Eq. A-11). The integration of both terms over the radial region of radius R gives the relation between the conduction-heat

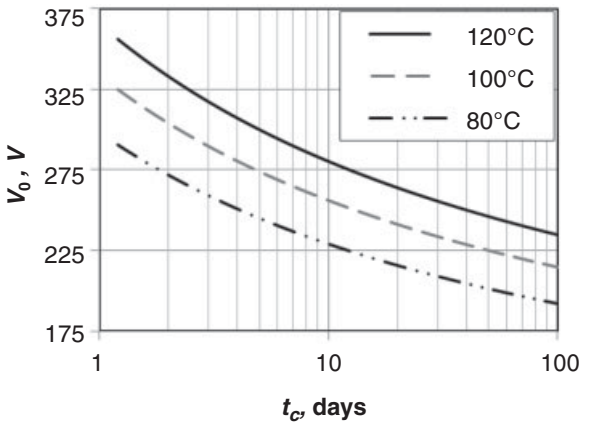

Fig. 4—Time of conduction-heating domination t_c for different electrode temperatures given by ΔT (in legend).

flux, which enters the region bounded internally by the electrode at imposed constant temperature $\Delta T = T_l - T_0$ [an analytical solution can be found in Carslaw and Jaeger (1959)] and early-time Joule's total power inside the electrically uniform region; for details, see Appendix A.

The voltage-vs.-time graphs in **Fig. 4** present the conditions where the heat conduction dominates—namely, in the region below the curves. Starting from any point on any curve, at higher voltages or longer times, Joule's power becomes more important. It seems that optimal early-time heating may combine reduced voltage and the conduction heat-transfer application.

Numerical Methodology

The STARS reservoir simulator has been used to model LFH for different geometrical configurations, initial reservoir conditions, and well/electrode parameters. We used this simulator to model multicomponent thermal flow and, particularly, to estimate the oil recovery in the case of the LFH application using the so-called electric module. STARS offers a bulk electric-conductivity model on the basis of a generalized Archie's law (Eq. 3) and complex potential definition capable of giving the potential and phase conditions, which correspond, for example, to three-phase electric-power supply. Evidently, the case to study was not trivial for numerical consideration: first, because of the great viscosity of bitumen; second, because of the large electric-conductivity ratio of initial and injected fluids; and, finally, because of the peculiar local circulation-flow pattern around electrodes and production wells. Despite this, the simulations have been successful and the results can be taken as reliable. Two models have been used systematically for testing and principal computations (see Fig. 1). Both were 3D with overall no-flow boundary conditions (and, thus, with no heat losses), the main difference being geometry (Cartesian for Fig. 1a and cylindrical for Fig. 1b) and number of wells/electrodes used. The particular numerical problems that have been encountered during our study are considered in more detail later.

Gridblock-Size Limitations. The Joule's heating power field around the electrode is nearly singular, and care should be taken to make the numerical results more precise in the electrode vicinity. Another important factor is the computation of a high-conductivity-zone configuration related to the injected-brine circulation and, more specifically, to the injected-salt distribution in the reservoir. Because of numerical dispersion, a certain amount of salt can propagate faster and, hence, the high-conductivity zone can penetrate farther than it would without this numerical artifact. To manage both factors for our STARS model, the only effective means is gridblock-size limitation. **Fig. 5** illustrates the numerical-dispersion effect on total Joule power in the computational region ($R = 8$ m). Four uniform grids have been used, with gridblock sizes (in the radial direction) indicated in the figure legends (e.g., $R/10$, $R/20$). An evident smearing effect of the salt-concentration profiles results in total-power (and, thus, temperature-field) deviation. Finally, for the base-case 3D region, the 41×35×33 grid has been chosen with gridblock size of approximately 0.4 m in each direction. The region dimensions (L, W, and H) are specified in **Table 1.**

Timestep Limitations. Nearly pointwise injection of highly conductive-fluid ("highly" in the sense of conductivity contrast between reservoir and injected fluid) may cause convergence problems, especially at the initial stage of the process. The nonlinear solver has been complaining frequently during the computation of the Jacobian (i.e., has reported a significant fraction of nonlinear iteration), which had remained nonconverged during timestep computations. The proper choice of the solver-tuning parameters can help greatly, but it is not a universal remedy. The most powerful means turned out to be the timestep limitations, which are user defined and are to be imposed explicitly. The optimal choice of timestep allows for complete avoidance of the nonlinear solver messages. For the base case under consideration, the timestep was approximately 1 day (after a few shorter timesteps).

Constant-Conductivity Tests. In the course of the model verification, a comparison to available analytical solutions for an electrically uniform reservoir has been performed. The first case of countercurrent LFH for single-phase flow in a radial region around an electrode, which simultaneously was used like a production well, was reported in Bogdanov et al. (2008). Also, the available

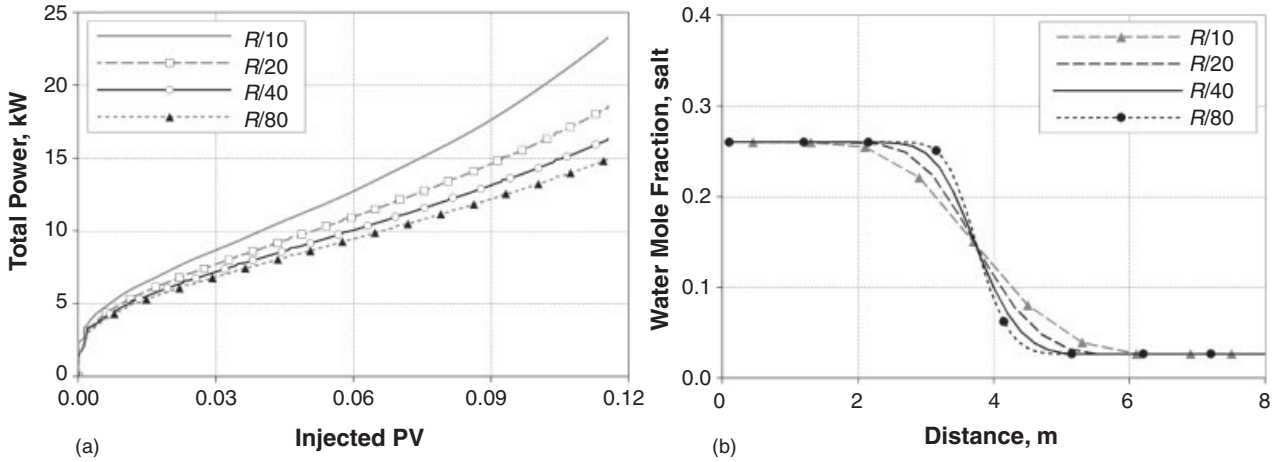

Fig. 5—Instanteneous total Joule's power during saltwater injection by means of an electrode (at 10 m³/d) for different grids (a) and concentration profiles after 90 days of injection; a 3D radial model with partially penetrated electrode was used (see Fig. 1b).

TABLE 1—RESERVOIR AND INJECTION PARAMETERS		
Parameter	Value	Units
Length (L)	13.9	m
Width (W)	16	m
Height (H)	12	m
Porosity	35	p.u.
Permeability	3000	md
Rock volumetric heat capacity	2.2×10^{6}	$J/m^3/K$
Oil initial viscosity	1000.26	Pa·s
Injection pressure	1.5×10^{6}	Pa
Initial reservoir pressure	0.8×10^{6}	Pa
Initial reservoir temperature	10	°C
Initial water saturation	20	%
Effective initial reservoir salt concentration	0.5	wt%
Effective injected brine salt concentration	5	wt%
Initial bulk electric conductivity	0.005	S/m

transient solutions for the temperature field during preheating (without fluid flow) and LFH-assisted waterflooding around a single electrode have been used for the purpose of testing numerical results (Bogdanov and Kamp 2009). The constant-conductivity tests have shown good agreement between theoretical and numerical results.

Numerical Performance of the Model. The base-case computations with chosen numerical-model parameters presented in **Tables 1 and 2** were performed using 47,355 gridblocks (i.e., on the 41×35×33 grid). The computation of the first 100 days of preheating (without production) took 20 minutes of computation. After that, the computation of 720 days of the production period took a few hours.

Main Results and Discussion

The LFH simulations have mainly been performed using the same 3D region geometry (Fig. 1) that is constructed on the basis of the reported well/electrode pattern (McGee and Vermeulen 2007). Generally, two periods can naturally be distinguished for each case: the preheating period and the production period. During the first period, the original bitumen is heated without production to reach the proper mobility condition for subsequent recovery. The production results depend much on the bitumen viscosity and, hence, on the reservoir temperature field at the end of the preheating period. Once the proper condition is reached, the production can be started using, for instance, a suitable conventional method of heavy-oil recovery. The electrical heating, however, is normally continued during production, at least part of the time.

Preheating. Besides the electric-current supply to the reservoir, the preheating process includes the brine recirculation near the electrodes. The salt water is injected from both ends of the electrodes and is withdrawn in the middle; see **Fig. 6.** The convective heat transfer contributes to more-homogeneous heating and transporting of the dissolved solute destined to modify the bulk electric conductivity around the electrode. This dual effect leads to more-effective and more-powerful heating (per unit of electric potential applied).

The factors affecting the preheating are numerous and include not only the injection-well and brine parameters but also the porous-medium and fluid properties, especially very near the electrodes. For example, after the water breakthrough to the electrode middle point, which is relatively fast, the brine will circulate inside a limited volume around the electrode. This part of the reservoir, with elevated water saturation and the solute concentration corresponding to that in the injected brine, can be called a circulation chamber. From a physical viewpoint, the circulation chamber acts like an effective electrode because of the high electric conductivity inside it, which is because of three physical factors—water saturation (conventional Archie's law), solute concentration, and temperature (Eq. 3). Obviously, the shape evolution of the chamber will depend on factors such as porous-medium transport properties, reservoir compressibility, phase mobilities and their variation with the electric field because of the electroviscous effect [see, for example, Onsager and Fuoss (1932)], and the physical parameters of phenomena such as capillary imbibition and convective dispersion. Not all of these factors are equally important in each particular case; however, each of them may contribute to the preheating, as has been shown.

It was not our purpose to present a comprehensive overview of factors influencing the brine-assisted electrical preheating. Even so, there exist among them a few parameters that can be controlled through the wells. To define such injection parameters, such as the salt concentration, the solution temperature, and the injector/producer conditions during this period, sensitivity studies have been carried out. The initial oil viscosity is very high, and, obviously, the brine injection is practically possible only after some elevated reservoir temperature is reached and continues to grow in the electrode vicinity. Subject to reservoir properties and electric-power limitations, it may be feasible to start with conductive heating for a first short period of preheating.

Brine Concentration and Temperature. It is well known that the electric conductivity of brine depends crucially on the solute

TABLE 2—ROCK AND FLUID PROPERTIES USED BY NUMERICAL MODELS					
Component	Phase	Density (kg/m^3)	Thermal Expansion Coefficient (K^{-1})	Compressibility Coefficient (kPa^{-1})	Thermal Conductivity Coefficient (J/m/K/d)
Oil	Bitumen	1010	2.66×10^{-4}	4.57×10^{-7}	1.84×10^{4}
Water	Aqueous	998	7.85×10^{-4}	6.84×10^{-7}	6.83×10^{4}
Salt	Aqueous	998	7.85×10^{-4}	6.84×10^{-7}	6.83×10^{4}
Rock	Solid	–	–	3.45×10^{-7}	1.8×10^{5}

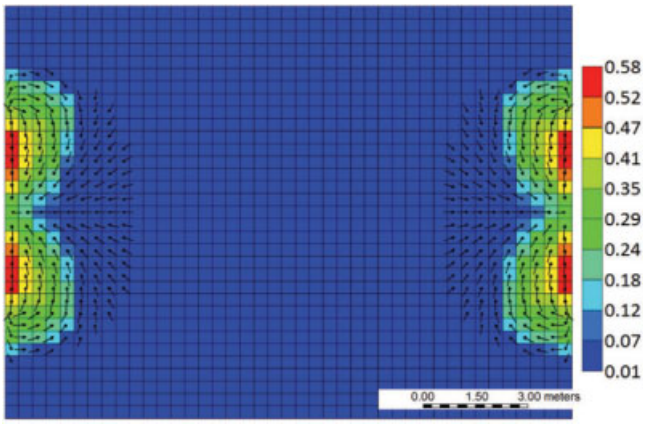

Fig. 6—Bulk-reservoir-electric-conductivity field and water-circulation local direction (black arrows) around Electrodes A and B (see Fig. 1) after 60 days of brine recirculation. The water is injected at both ends, and is produced in the middle, of each electrode.

concentration. The injection of such a fluid may lead to increasing bulk reservoir conductivity locally by a factor of approximately 100 (Fig. 6). This effect is also because of the water-saturation rise, especially near the electrode. The preheating temperature fields presented in **Fig. 7** and, particularly, the total-power/time diagrams shown in **Fig. 8** demonstrate that the effect of the solute concentration is not linear and at some typical concentration it becomes relatively small. At the same time, the hot brine injection does not have an effect as significant as might be expected because, at conditions under which the injection becomes possible, the temperature is already high enough near the electrode. It can be seen easily that, although the concentration and temperature effect are common, their optimal values depend on many factors and should be defined independently for each particular case.

Well-Pressure Conditions. Because of the injectivity problem at initial reservoir conditions, to provide the brine recirculation in the near-electrode region, pressure conditions are given at electrode wells. After a relatively short period, the pressure condition can be replaced by that of an injection rate, which has a very small impact on main-process parameters (except for the water injection, of course). The water injection for electrode-temperature regulation should be maintained during total heating time to avoid significant water evaporation. Note that, independently of the formation-fracture pressure, the injection pressure has another limit related to the gradually diminishing effect of the pressure rise on the preheating temperature field. According to sensitivity-test results, the injection pressure has been chosen equal to 15 bar.

Base Case. The main properties and parameters for the base preheating case are summarized in Table 2 and Fig. 2. They comprise particularly the reservoir and fluid properties and the brine-injection conditions. Because the main objective in this stage is the homogeneously heated reservoir, a general indicator of successful preheating is the mean reservoir temperature, which is proportional to the total amount of thermal energy generated in the reservoir. The electric-power supply can provide the necessary amount of energy within certain limits, which may include applied-voltage or total-current (i.e., total-power) limitations. In the base case, the electric current is injected to provide a given total power of 30 kW or, in other words, 2.5 kW per 1 m of region thickness. Note that, in view of the symmetry boundary conditions on the lateral sides (Fig. 1a), the region is composed of 1 electrode and 1 production well so that the total power condition implies a total power of 30 kW per electrode. At the given total power, the mean reservoir TRR is 0.43°C/d.

From the beginning of power supply, the magnitude of potential on the electrodes varies with time **(Fig. 9)** and indicates a significant and rather rapid variation of mean reservoir conductivity. This clearly demonstrates that the brine circulation around electrodes is helpful in the bulk-conductivity modification. The salt concentration indicates the circulation-chamber boundaries around electrodes, which are simultaneously the limits of elevated-conductivity zones. Inside these zones, both the potential variation and the mean heating power are relatively small so that the major part of heating power is put outside them.

Production. From the production viewpoint, the LFH practical application may have additional restrictions with respect to conventional thermal improved-oil-recovery methods. Besides the reduced spacing between electrodes, the choice of well/electrode pattern is limited because the electrode pattern should follow the base element triangular shape. Evidently, this is not the case for direct-current power supply, which does not have such limitation. Again, more wells can be used for production purposes so that, in principle, not all wells must participate directly in power distribution in the reservoir. The latter gives a new degree of freedom for the well-pattern design.

Another restriction deliberately taken for the current work is the two-phase-flow framework, which avoids the consideration of steam generation during LFH. Although it might be advantageous under certain conditions to evaporate the water partially, the idea seems technically delicate and dubious, with an advantage yet to be proved.

The base-case computations show that, after a preheating period, which may last a few months or more, the mean temperature in

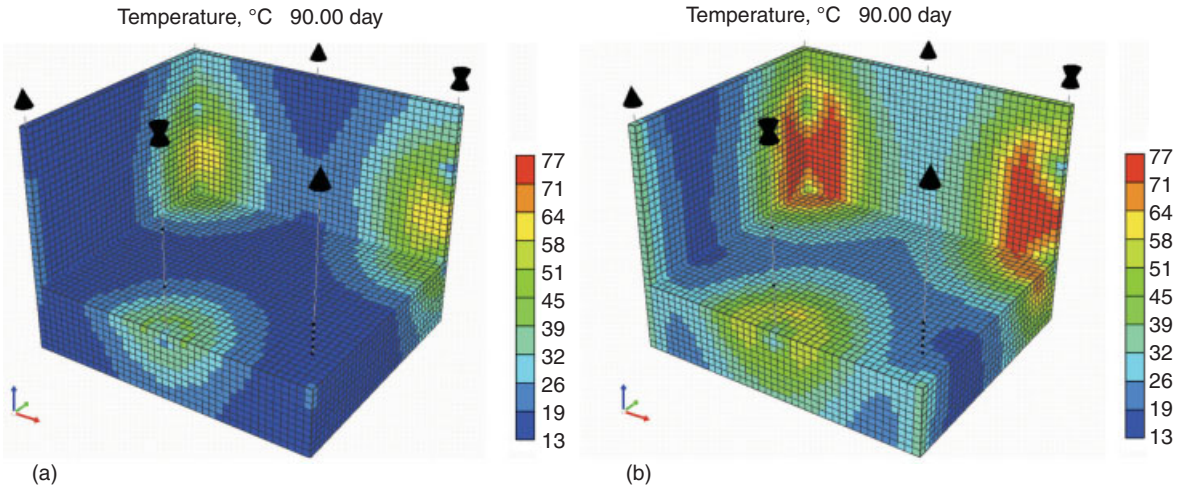

Fig. 7—Temperature field after 3 months of preheating assisted by cold-water injection with initial reservoir salt concentration (a) and base-case 5 wt% salt concentration (b). Applied-potential magnitude is 312 V.

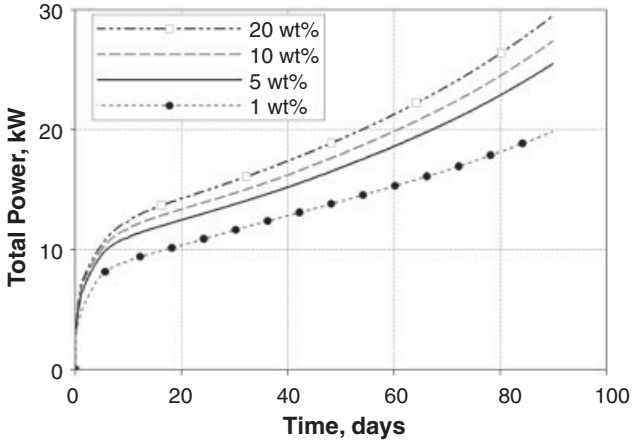

Fig. 8—Influence of the injected-brine concentration in the circulation chamber on the total heating power in the computational region.

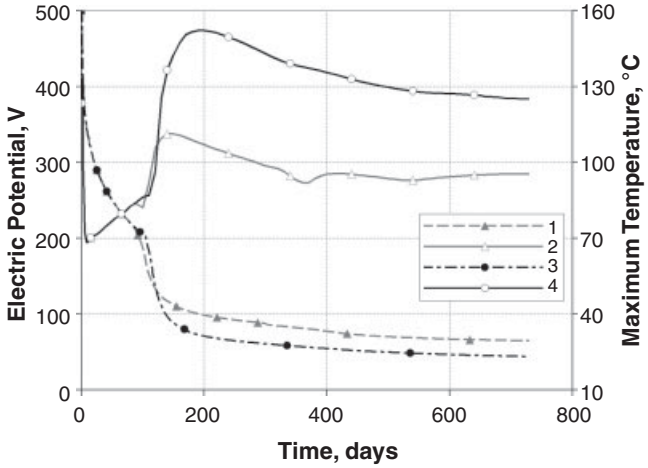

Fig. 9—Variation of the applied-electric-potential magnitude (1, 3) and the temperature maximum (2, 4) during preheating/production at constant total power (30 kW). The production started after 85 days (gray lines) and 105 days (black lines) of preheating.

the reservoir rises and reduced bitumen viscosity allows for use of a conventional improved-oil-recovery method for oil production, in combination with LFH or not. The combination of LFH with hot-water injection is probably the most promising option for the production. As usual, the sweep efficiency and the energy expenses per unit of produced oil are of major importance at this stage.

At the end of the preheating period, the typical temperature field shown, for instance, in Fig. 7b is composed of less-heated zones, which correspond to local minima of the power field (see the lowest power zones in Fig. 1a in dark blue and magenta between Production Wells 2 and 3 and Electrodes A and B, respectively). Consequently, the preferable flow direction, which follows the local temperature elevation, is B–1–A (or, equally, 3–C–2); see Fig. 1a. To provide better sweep efficiency during production, either the injected water is to be distributed uniformly from the very beginning or, after the water breakthrough from the nearest electrodes, the flow direction should be turned (i.e., half of all production wells should be converted to injection wells).

As for energy/oil ratio, it depends mainly on total heating time and its appropriation. The choice to make is between the preheating-period duration (and, hence, the mean reservoir temperature at the beginning of production) and the heating time at the production stage.

The main results for two possible production scenarios are shown in **Figs. 9 and 10.** The main difference between them is that, in the first case, the production started after 85 days of preheating (results shown in gray lines in Figs. 9 and 10), while, in the second case, it was after 105 days of preheating (results shown in black lines). At production, the bottomhole pressure of 500 kPa is given at each production well in both cases. Another difference between the two production scenarios is in the time and the way Production Wells 2 and 3 (Fig. 1) were converted to injection wells. In the first case, it happened after 300 days and the cold water has been injecting from all injection wells. In the second case, after 170 days, the production wells have been converted to hot-water-injection sites (T_I = 80°C).

The electrical heating with maximum power of 30 kW and the water recirculation at constant pressure was continuing at this step. The electric field did not change much in the two cases; the potential vs. time diagrams are rather close (Fig. 9). However, the temperature was different because of additional heating time and the hot water injected in the second case. The variation of temperature maximum in the reservoir shows a difference of approximately 30°C (Fig. 9). Consequently, the oil-production rate reached 1.36 m^3/d after approximately 116 days of heating in the second case and was significantly higher than that for the first scenario (Fig. 10). For approximately 2 months, the production rate continued to be relatively high. The production was conducted for 2 years, and, after this time, the best recovery factor was approximately 35% (or approximately 260 m^3 of oil produced; the initial amount of oil in place was 747.3 m^3 at reservoir conditions). However, the total water injection has been higher in this case.

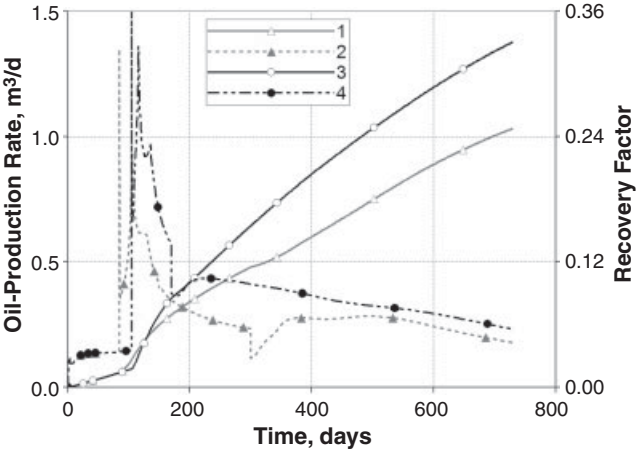

Fig. 10—Recovery factor (1, 3) and oil-production rate (2, 4) for 2 years of the LFH. The production started after 85 days (1, 2) and 105 days (3, 4) of preheating. The well conversion is performed at 300 days (1, 2) and 170 days (3, 4).

Conclusions

- The most important physical properties affecting the LFH results are the bulk reservoir electrical conductivity, the reservoir temperature, the initial oil viscosity, the fluids, and the reservoir thermal and transport properties. The main operational conditions are the applied-power limit, injected-brine electrical properties, the electrode spacing, and the injection-pressure limit. All these data were collected carefully from the literature.
- The STARS simulator is capable of properly simulating the electrical heating coupled with the saltwater circulation in 3D radial and Cartesian geometries. The simulations have been performed on a carefully selected grid without apparent problems.
- Saltwater circulation may significantly improve both the bulk electric conductivity and the power distribution during the preheating and at least the early production periods. The electric-power supply can be provided at lower electric potential, which certainly may facilitate and enhance the LFH application. Furthermore, the water circulation increases the convection heat

transfer around the electrodes and helps manage hot spots in the vicinity of the electrodes.

- A recovery factor of approximately 35% has been reached after 2 years of production. The process time is a function of electric power that can be supplied for heating. The production may be improved by extending the preheating period.

Nomenclature

C_R = reservoir volumetric heat capacity, m/t²LT, J/(m³·K)
E = electric field, mL/qt², V/m
F = reservoir formation factor, dimensionless
G = dimensionless conductance factor, dimensionless
G_0 = dimensionless conductance factor for a homogeneous medium, dimensionless
H = thickness of 3D Cartesian model, L, m
J = total electric current per unit of the electrode length, q/Lt, A/m
L = length of 3D Cartesian model, L, m
m = power in Archie's law for electric conductivity, dimensionless
P = local electric-power density, m/t³L, W/m³
P_0 = power-density magnitude, m/t³L, W/m³
P_{LF} = local electrical-heating power density, m/t³L, W/m³
P_{tot} = total power supply per unit of the electrode length, mL/t³, W/m
q_C = conduction heat flow per unit of electrode length,m/t³, W/m²
Q = volumetric injection rate per unit of the reservoir thickness, L²/t, m³/(m·s)
Q_f = convective-heat-transfer parameter, mL/t³T, W/(m·K)
r = distance, L, m
r_0 = electrode-well radius, L, m
r_1 = size of elevated-conductivity zone, L, m
R = 3D-radial-model horizontal size, L, m
S_w = water saturation, dimensionless
t = time, t, seconds
t_C = time of conduction-dominating heating, t, seconds
T = temperature, T, K
T_I = electrode-well temperature, T, °C
T_0 = initial reservoir temperature, T, °C
U_f = convective-heat-flux parameter, m/t³T, W/(m²·K)
V_0 = electric-potential input given at the electrode, mL²/qt², V
V_C = electric potential magnitude in Eq. A-17, mL²/qt², V
W = width of 3D Cartesian model, L, m
x = space variable, L, m
Z = dimensionless parameter in Eq. A-16, dimensionless
α = lithology parameter in Archie's law, dimensionless
γ = Euler's constant, dimensionless
θ = dimensionless temperature, dimensionless
Θ = dimensionless average temperature, dimensionless
κ = electric conductivity factor in composite-medium model, dimensionless
K = heat-conduction coefficient, mL²/t³LT, W/(m·K)
Λ = effective electric conductance per unit of thickness, q²t/L³m, S/m
ν = electric-potential variable, mL²/qt², V
Π = thermal Péclet number, dimensionless
ρ = dimensionless distance from the electrode well, dimensionless
ρ_0 = dimensionless electrode radius, dimensionless
ρ_1 = dimensionless size of elevated-conductivity zone, dimensionless
σ = bulk electric conductivity of reservoir, q²t/L³m, S/m
σ_0 = initial electric conductivity of the reservoir, q²t/L³m, S/m
σ_w = water-phase electric conductivity, q²t/L³m, S/m
τ = dimensionless time, dimensionless
τ_0 = typical dimensionless time for thermal conductivy, dimensionless
ϕ = porosity, dimensionless

Acknowledgments

Total S.A. is acknowledged for sponsoring research activities and for allowing the results to be published. Karima el Ganaoui is acknowledged for carrying out preliminary reservoir simulations.

References

Archie, G.E. 1942. The Electrical Resistivity Log as an Aid in Determining Some Reservoir Characteristics. SPE-942054-G. *Trans.,* AIME, **146:** 54–62.

Bogdanov, I.I. and Kamp, A.M. 2009. Analytical and Numerical Modeling of Electrical Heating Method for Oil Recovery. *Proc.,* 3rd International Conference on Approximation Methods and Numerical Modelling in Environment and Natural Resources (MAMERN '09), Pau, France, 8–11 June, Vol. 1, Paper MS01-2, 263–268.

Bogdanov, I.I., El-Ganaoui, K., and Kamp, A.M. 2008. Study of Electrical Heating Application for Heavy Oil Recovery. Presented at COMSOL Conference 2008, Hannover, Germany, 4–6 November.

Carslaw, H.S. and Jaeger, J.C. 1959. *Conduction of Heat in Solids*, second edition. Oxford, UK: Oxford University Press.

El-Feky, S.A. 1977. Theoretical and Experimental Investigation of Oil Recovery by the Electrothermic Technique. PhD dissertation, University of Missouri—Rolla, Rolla, Missouri.

Harvey, A.H., Arnold, M.D., and El-Feky, S.A. 1979. Selective Electric Reservoir Heating. *J Can Pet Technol* **18** (3): 47–57. JCPT Paper No. 72-03-04. doi: 10.2118/79-03-04.

Hiebert, A.D., Vermeulen, F.E., and Chute, F.S. 1989. Application of Numerical Modeling to The Simulation of the Electric-Preheat Steam-Drive (EPSD) Process In Athabasca Oil Sands. *J Can Pet Tech* **28** (5): 74–86. JCPT 89-05-07. doi: 10.2118/89-05-07.

Hiebert, A.D., Vermeulen, F.E., Chute, F.S., and Capjack C.E. 1986. Numerical Simulation Results for the Electrical Heating of Athabasca Oil-Sand Formations. *SPE Res Eng* **1** (1): 76–84. SPE-13013-PA. doi: 10.2118/13013-PA.

Jones, G. and Dole, M. 1929. The Viscosity of Aqueous Solutions of Strong Electrolytes with Special Reference to Barium Chloride. *J. Am. Chem. Soc.* **51** (10): 2950–2964. doi: 10.1021/ja01385a012.

Killough, J.E. and Gonzalez, J.A. 1986. A Fully-Implicit Model for Electrically Enhanced Oil Recovery. Paper SPE 15605 presented at the SPE Annual Technical Conference and Exhibition, New Orleans, 5–8 October. doi: 10.2118/15605-MS.

McGee, B.C.W. 2008. Electro-Thermal Pilot in the Athabasca Oil Sands: Theory Versus Performance. *World Oil* **229** (11): 47-54.

McGee, B.C.W. and Vermeulen, F.E. 2007. The Mechanisms of Electrical Heating for the Recovery of Bitumen From Oil Sands. *J Can Pet Technol* **46** (1): 28–34. JCPT No. 07-01-03. doi: 10.2118/07-01-03.

Onsager, L. and Fuoss, R.M. 1932. Irreversible Processes in Electrolytes. Diffusion, Conductance and Viscous Flow in Arbitrary Mixtures of Strong Electrolytes. *J. Phys. Chem.* **36** (11): 2689–2778. doi: 10.1021/j150341a001.

Pizarro, J.O.S. and Trevisan, O.V. 1990. Electrical Heating of Oil Reservoirs: Numerical Simulation and Field Test Results. *J Pet Technol* **42** (10): 1320–1326. SPE-19685-PA. doi: 10.2118/19685-PA.

Todd, J.C. and Howell, E.P. 1978. Numerical Simulation Of In-Situ Electrical Heating To Increase Oil Mobility. *J Can Pet Technol* **17** (2): 31–41. JCPT Paper No. 78-02-01. doi: 10.2118/78-02-01.

Ucok, H., Ershaghi I., and Olhoeft, G.R. 1980. Electrical Resistivity of Geothermal Brine. *J Pet Technol* **32** (4): 717–727. SPE-7878-PA. doi: 10.2118/7878-PA.

Wittle, J.K., Hill, D.G., and Chilingar, G.V. 2008. Direct Current Electrical Enhanced Oil Recovery in Heavy-Oil Reservoirs to Improve Recovery, Reduce Water Cut, and Reduce H_2S Production While Increasing API Gravity. Paper SPE 114012 presented at the SPE Western Regional and Pacific Section AAPG Joint Meeting, Bakersfield, California, USA, 29 March–2 April. doi: 10.2118/114012-MS.

Appendix A—Analytical Model of Preheating for Composite Medium

A complete mathematical model of an electrical-heating problem accounting for electrothermal-fluid dynamic aspects of oil production should include the electric-field (EF) description, and component-mass- and total-thermal-energy-conservation equations. From a mathematical-modeling viewpoint (and, according to the physical description presented in the body of the paper), the solution of the EF equation provides a right-hand-side term to the thermal-energy-conservation equation. Evidently, the EF propagation is much faster than any other physical field in the reservoir, so the heating-power distribution can be taken as a stationary field, which immediately matches any variation of other physical fields. In other words, the time derivatives in the EF equations can be dropped and the stationary heating-power term, depending on the spatial variable, will vary in time; but, this is a parametric dependency because of the evolution of the reservoir electric properties.

Here, the determination of the heating term will be made for one particular case of electrical-property variation—namely, for the so-called composite medium. This enables us to reduce the problem to one equation and to obtain useful solutions for practically important problems.

LFH-Term Model: 1D Radial Case. Consider the EF equation for a 1D radial case of LFH. Combining the (stationary) electric-charge-conservation equation with Ohm's law, the electric-potential equation can be written as

$$-\nabla_r \cdot \left(\sigma \nabla_r \upsilon\right) = 0, \quad \text{(A-1)}$$

where σ is the reservoir bulk electric conductivity, υ is electric potential, $r_0 \le r \le R$ in the distance from the electrode center, and the subscript r denotes the radial part of corresponding differential operator; $\upsilon(r_0) = V_0$, $\upsilon(R) = 0$. Archie's law (Eq. 3) specifies the variation of reservoir electric conductivity with water saturation and temperature. The water conductivity σ_w depends also on water-phase composition.

The solution to Eq. A-1 is the particular expression of Ohm's law written for a given geometry:

$$-r \cdot \sigma \cdot \partial_r \upsilon = J/2\pi. \quad \text{(A-2)}$$

Here, J is electric current per unit thickness, *A/m*; note also that the notation $\partial_x(\cdot)=\partial(\cdot)/\partial x$ is used, which applies for any variable x. It follows from Eq. A-2 that, generally speaking, J is time dependent, $J = J(t)$ because $\sigma = \sigma(t)$ (the temperature, the water saturation, and the salt concentration vary during the heating), while Eq. A-1 does remain stationary. Integrating Eq. A-2 between internal (r_0) and external (R) radii, one obtains an upscaled Ohm's law, which defines the electric current at given potential V_0 applied between internal and external radii:

$$J = V_0 \Lambda. \quad \text{(A-3)}$$

The effective conductance Λ is determined by weighted harmonic average of local electric-conductivity field:

$$\Lambda = 2\pi \Big/ \int_{r_0}^{R} \frac{\mathrm{d}r}{\sigma r}. \quad \text{(A-4)}$$

Finally, the heating power density, which is defined as

$$P = \sigma \left|\nabla_r \upsilon\right|^2, \quad \text{(A-5)}$$

can be determined from Eqs. A-2 and A-3:

$$P(r) = \sigma \cdot \left[\frac{V_0 \Lambda}{2\pi r \sigma(r)}\right]^2. \quad \text{(A-6)}$$

Take a reference conductivity σ_0, the problem size R, and the applied potential V_0 as characteristic scale values. Then, Eq. A-6 can be expressed in the following form:

$$P(r) = P_0 \cdot \frac{\sigma_0}{\sigma(r)} \cdot \left(\frac{GR}{r}\right)^2, \quad \text{(A-7)}$$

where

$$P_0 = \frac{\sigma_0 V_0^2}{R^2},$$

$$G = \frac{\Lambda}{2\pi\sigma_0} = \left(\int_{\rho_0}^{1} \frac{\sigma_0 \mathrm{d}\rho}{\sigma\rho}\right)^{-1},$$

$$\rho = r/R. \quad \text{(A-8)}$$

Note that P_0 in Eq. A-7 is a dimensional parameter representing a characteristic power magnitude. The dimensionless parameter G accounts for reservoir electric-conductivity distribution $\sigma(\rho)$ (Eq. A-8). The total heating power P_{tot} per unit of thickness can be found by means of integration of Eq. A-7 over the problem region. This gives the following expression:

$$P_{tot} = 2\pi R^2 P_0 G, \quad \text{(A-9)}$$

which shows that dimensionless conductance factor G, depending on electric-conductivity distribution, defines also a total power release. Note that, for a homogeneous medium (i.e., at $\sigma = \sigma_0$), the factor depends only on $\rho_0 = r_0/R$.

Dimensionless Conductance Factor for Composite Medium. According to modified Archie's law (Eq. 3), the bulk electric conductivity σ depends on local water saturation, solute concentration, and temperature. So the concentration or temperature rise and the water-saturation increase because of, for instance, water injection may lead to significant variation of bulk electric conductivity around an electrode.

In this subsection, a composite-medium model with piecewise-constant bulk electric conductivity is considered:

$$\sigma(\rho) = \kappa\sigma_0, \ \rho_0 \le \rho \le \rho_1$$

and

$$\sigma(\rho) = \sigma_0, \ \rho_1 < \rho, \quad \text{(A-10)}$$

where κ and ρ_1 are the model parameters. The case $\kappa > 1$ is addressed here because only increasing conductivity around an electrode allows for enhancing the heating power in the reservoir (per unit of applied potential). Start with the definition of factor G, which reads now as

$$G(\rho_0, \rho_1, \kappa) = \left(\int_{\rho_0}^{1} \frac{\sigma_0 \mathrm{d}\rho}{\sigma\rho}\right)^{-1} = \left[\frac{1}{\kappa}\ln(\rho_1/\rho_0) + \ln(1/\rho_1)\right]^{-1}. \quad \text{(A-11)}$$

Parameter G defines also the total power (Eq. A-9). To illustrate the influence of the elevated-conductivity zone on total power and, thus, on average heating rate, the ratio G/G_0 as a function of the size ρ_1 is presented in Fig. 3; here, G_0 is the conductance factor for a uniform medium, $G_0 = G(\kappa = 1) = 1/\ln(1/\rho_0)$. The ratio G/G_0 can be used directly to estimate the total heating acceleration according to elevated-conductivity propagation.

It can be seen easily from Fig. 3 that, at $\kappa > 10$, the factor G depends mainly on ρ_1 and only slightly on κ. At high enough conductivity, it is close to the asymptotic curve ($\kappa = \infty$) shown by a dashed black line. It follows from Eq. A-11 that, at this limit, $G = 1/\ln(1/\rho_1) = G_0(\rho_1)$, or, in other words, the factor G for this case corresponds to a uniform-medium factor but with the electrode of radius ρ_1 instead of ρ_0.

Thermal-Energy Balance: Model Equation. The local-power-density term $P(r)$ appears in the right-hand side of the thermal-energy-conservation equation, which, for homogeneous fluid flow, may be written, for instance, as

$$C_R\partial_t T + U_f\nabla_r T - \nabla_r\cdot\left(\mathrm{K}\cdot\nabla_r T\right) = P(r), \quad \ldots\ldots\ldots\ldots\ldots\ldots (A\text{-}12)$$

where $Q_f = C_f Q = 2\pi r U_f$, C_f is injected-fluid volumetric heat capacity, and C_R is reservoir (bulk) volumetric heat capacity. Note that the assumption of fluid homogeneity means here that the phase volumetric heat capacities are the same. In case of steady fluid flow $2\pi r U_f = Q_f$ = constant, so $U_f \propto r^{-1}$. Unless otherwise stated, the model under consideration involves constant parameters C_R, K, and U_f. The corresponding dimensionless equation is based on the following dimensional characteristic values—temperature $T_D = P_0 R^2/\mathrm{K}$; power P_0 determined from Eq. A-8; time $t_D = C_R R^2/\mathrm{K}$; and length R—and reads as

$$\partial_\tau\theta + \Pi\rho^{-1}\partial_\rho\theta - \rho^{-1}\partial_\rho\left(\rho\partial_\rho\theta\right) = \zeta(\rho). \quad \ldots\ldots\ldots\ldots\ldots\ldots (A\text{-}13)$$

Here, $\theta = (T - T_0)/T_D$ is the dimensionless temperature variable, $\Pi = Q_f/(2\pi\mathrm{K})$ is the thermal Péclet number, and, according to Eq. A-7, $\zeta(\rho) = (\sigma_0/\sigma)\cdot(G/\rho)^2$.

Eq. A-13 indicates two principal parameters of the model, the Péclet number Π and the effective-conductance factor G, which has been discussed (Eq. A-11). The third model parameter is the electrode radius ρ_0. However, for a homogeneous medium, the dimensionless conductance factor is not an independent parameter because it depends only on ρ_0 (Eq. A-11). The equation for average temperature variation can be found easily from Eq. A-13. Multiplying it first by differential areal element $\rho\cdot\mathrm{d}\rho$ and integrating then between internal ($\rho = \rho_0$) and external ($\rho = 1$) radii, one obtains

$$\partial_\tau\Theta = 2\left(G + \Pi\theta^0\right)\Big/\left(1 - \rho_0^2\right), \quad \ldots\ldots\ldots\ldots\ldots\ldots (A\text{-}14)$$

where the average temperature and the temperature drop are defined as

$$\Theta = \frac{2}{1-\rho_0^2}\int_{\rho_0}^{1}\theta\rho\mathrm{d}\rho$$

and

$$\theta^0 = \theta\left(\rho_0\right) - \theta(1), \quad \ldots\ldots\ldots\ldots\ldots\ldots (A\text{-}15)$$

respectively. Make an estimation of the right-hand-side term in Eq. A-14. Injection of water at $T^0 = 90°\mathrm{C}$, with a rate of 1 m^3/d per electrode of 6-m length and the electric-power supply at potential input $V_0 = 300$ V; also the bulk reservoir conductivity $\sigma_0 = 0.005$ S/m, $\rho_0 = 0.0125$, and the heat-conduction coefficient K = 2 W/(m·K) makes $\Pi\theta^0 \approx G \approx 0.23$. Thus, the total mean power is approximately 7.4 $\mathrm{W/m}^3$ or, at $C_R = 2.6\times10^6$ $\mathrm{J/(m^3\cdot°C)}$, the mean rate of the reservoir temperature rise is 0.25°C/d. Note that, at given parameters, the contributions of Joule's power and hot-water injection are the same. Let it be mentioned in passing that being positive at the preheating stage, the temperature θ^0 may become negative during production.

Conduction-Dominating Period. Consider the pure conductive heating around an infinite electrode by keeping it at a constant high-enough temperature T_I. Then, at time $\tau_0 = \nu t/\rho_0^2 >> 1$, where $\nu = K/C_R$, the conductive-heat flow (per unit of electrode length) is given by (Carslaw and Jager 1959):

$$q_C = 4\pi\mathrm{K}\Delta T\left(Z - \gamma Z^2 - \ldots\right)$$

and

$$Z^{-1} = \ln\left(4\tau_0 - 2\gamma\right), \quad \ldots\ldots\ldots\ldots\ldots\ldots (A\text{-}16)$$

while the total Joule power (per unit of electrode length) is given by Eq. A-9. The heat-conduction flow drops with time, and, after some time t_C, which may be referred to as the conduction-dominating period, it becomes equal to P_{tot}. The potential magnitude defined from the condition $P_{\mathrm{tot}} = q_C$ as a function of t_C is shown in Fig. 4; there, $\rho_0 = 0.0125$, and the different values of the reduced electrode temperature $\Delta T = T_I - T_0$ are shown in the legend; the key parameter of this relation V_C reads as

$$V_C = \left(2K\Delta T/\sigma_0\right)^{1/2}. \quad \ldots\ldots\ldots\ldots\ldots\ldots (A\text{-}17)$$

For example, at K = 2 W/(m·°C), $\Delta T = 80°\mathrm{C}$, and $\sigma_0 = 0.005$ S/m, one obtains from Eq. A-17 that $V_C = 253$ V.

Igor Bogdanov has been a research engineer at the Open and Experimental Centre for Heavy Oil (CHLOE) in Pau, France, since 2006. He holds an MS degree in molecular and chemical physics and a PhD degree in fluid mechanics from the Moscow Institute of Physics and Technology, State University. Bogdanov worked for more than 10 years at the Institute for Problems in Mechanics of the Russian Academy of Sciences in Moscow. He continued his research in France, working for the Institute of Earth Physics in Paris for several years. Bogdanov is a member of SPE. **José Antonio Torres** has been a research engineer at CHLOE in Pau, France, since October 2007. He started working in the petroleum industry at VVA Consultores C.A., a Venezuelan company specializing in the field of consultancy in geomechanics. Later, Torres worked for PDVSA Intevep, mainly in the field of reservoir modeling and simulation. He holds a BS degree in chemical engineering and a one-year specialization degree in reservoir engineering, both from the Universidad Simón Bolívar, Venezuela, and a PhD degree in chemical and process engineering from the Universitat Rovira i Virgili, Taragona, Spain. **Hossein A. Akhlaghi** holds a BS degrees in petroleum reservoir engineering and in mechanical engineering from Sharif University of Technology, Tehran, Iran. He also holds a dual MS degree in reservoir engineering from the IFP School, Rueil-Malmaison, France, and the Petroleum University of Technology, Tehran, Iran. Akhlaghi carried out an internship at CHLOE from July to December 2009 on heavy-oil recovery enhanced by electrical heating. **Arjan Kamp** is the director of CHLOE, a research group affiliated with the University of Pau, France, and sponsored by Total. CHLOE carries out research on reservoir engineering aspects of heavy-oil-recovery methods. Kamp holds an MS degree in applied physics from Eindhoven University of Technology, The Netherlands, and a PhD degree in fluid mechanics from the University of Toulouse, Institut National Polytechnique, France. He is a member of SPE.